Uluslararası İleri Doğa Bilimleri ve Mühendislik Araştırmaları Dergisi
Sayı 7, S. 44-51, 3, 2023

Araştırma Makalesi

IJANSER

International Journal of Advanced Natural Sciences and Engineering Researches
Volume 7, pp. 44-51, 3, 2023

Research Article

https://as-proceeding.com/index.php/ijanser
ISSN: 2980-0811

Modeling of the Pore Shape Effect of the Plastic Behavior of Porous Materials

Mohamed Masmoudi[1*], Ilyas Bensalem[2], Wahid Kaddouri[3], Kaouther Bourih[4] and Abdellah Bourih[5]

[1,2,3,4,5] *Department of Mechanical Engineering, Laboratory of Mechanical Structures and Materials, Batna 2 University, Algeria*

[*]*(m.masmoudi@univ-batna2.dz) Email of the corresponding author*

(Received: 24 March 2023, Accepted: 2 April 2023)

(2nd International Conference on Engineering, Natural and Social Sciences ICENSOS 2023, April 4 - 6, 2023)

ATIF/REFERENCE: Masmoudi, M., Bensalem, I., Kaddouri, W., Bourih, K. & Bourih, A. (2023). Modeling of the Pore Shape Effect of the Plastic Behavior of Porous Materials. *International Journal of Advanced Natural Sciences and Engineering Researches*, 7(3), 44-51.

Abstract **–**Lotus-type porous materials are characterized by cylindrical porosities aligned along a single direction, giving them transverse isotropic behaviour with two independent effective properties. The first is a pore-parallel property that can be estimated by a simple law of mixtures. The second property, perpendicular to the pores, requires a homogenization calculation for its determination. The main purpose of this work is to estimate the effective tangent modulus of these materials by numerical homogenization based on the representative volume element. A formula allowing the estimation of the effective tangent modulus is proposed on the basis of the obtained numerical results which have shown that the shape of the pores has a great influence on the effective property studied. Its validation is ensured by its comparison with the various numerical results.

Keywords – Lotus-Type Porous Materials; Plastic Behavior; Tangent Modulus; Shape Effect; Numerical Homogenization

I. INTRODUCTION

The lotus-type porous materials are obtained via unidirectional solidification from a melt under hydrogen and argon atmospheres; their fabrication is well-controlled since they are manufactured by controlling the porosity, pore orientation, pore shape, and pore diameter. According to Nakajima [1], three different fabrication techniques for lotus-type porous metals are used: continuous casting, continuous zone melting and mold casting. The pore sizes are obtained by varying the solidification velocity and gas pressure. The solidification orientation controls the pore direction. The lotus-type porous materials techniques allow to produce metals, alloys, inter metallic compounds, semiconductors, and ceramics. Du et al. [2] investigated the effect of hydrogen and argon pressures on the structure of porous copper, including pore size, pores density, and porosity. The investigation demonstrated that increasing the gas, particularly hydrogen, pressure leads to an increase in pore density and a decrease in the pore size and porosity of the porous metal. Iio et al. [3] fabricated lotus-type porous aluminum by continuous casting technique in mixture gas of hydrogen and argon at various transfer velocities to elucidate the pore formation mechanism. Results indicated that a decrease in porosity with increasing transfer velocity in lotus-type aluminium is different from that reported for other lotus-type metals. However, the decrease in the average pore diameter with increasing transfer velocity is similar to that in other

lotus-type metals, such as stainless steel and copper. The anisotropic pore morphology of lotus-type porous materials (LTPMs) results in the anisotropy of their mechanical and physical properties. Several investigations have been carried out on the anisotropic properties of these materials [4-8].

In recent decades, the properties of LTPMs have been extensively investigated using various approaches. Ichitsubo et al. [5] explored elastic constants of lotus-type porous copper. A combination of resonance ultrasound spectroscopy and electromagnetic acoustic resonance methods has been used to determine the elastic constants of the composite. Moreover, this study demonstrated the validity of a micromechanics model which considers the matrix elastic anisotropy and the pore shape to calculate elastic constants of lotus-type porous metals. Hyun et al. [9] fabricated a lotus-type porous iron by the unidirectional solidification of the melt in a gas mixture of hydrogen (nitrogen) and argon. Results proved that the ultimate tensile and yield strengths of porous iron fabricated in a nitrogen atmosphere are approximately twice as high as those under a hydrogen atmosphere. Xie et al. [10] measured the damping constant of lotus-type porous magnesium with various porosities using the hanging excitation method. The damping constant was defined by an expression in terms of successive amplitude values of the damping wave and damping time. Nakajima [1] reviewed various properties of porous metals with directional pores, such as elastic property, electrical conductivity, the anisotropic behaviours of tensile, as well as the compressive and fatigue strength. Experimental results confirmed that these porous metals exhibit desirable sound absorption and vibration–damping properties. Effects of structural parameters on uni-axial tensile properties of Gasar porous copper were investigated by Zaijiu et al. [11]. Mathematical models and numerical simulations of the ultimate tensile strength were performed and confirmed by comparing results with experimental data. Recently, an optimal pore structure for maximum heat dissipation was reported by Liu et al. [12], which considered the effects of porosity, pore diameter, and open porosity on the heat transfer performance of a lotus copper heat sink. Chen et al. [13] measured the effective properties of a porous material with non-ellipsoidal concave pores. Their results indicated that geometrical parameters used in expressions for elastic moduli and conductivity are the same, and an across-property connection in such materials was established. Their study supports the hypothesis that irregularity factors affect elastic and conductive properties similarly. Considering the pore morphology effect, models for estimating effective thermal conductivities and ultimate tensile strengths of the lotus-type porous media were proposed by Kaddouri et al. [14] and Masmoudi et al. [15]. Their investigations showed that the pore shape exhibits a significant influence on the effective thermal conductivity, and the ultimate tensile strength. It was also showed that the pore shape has similar effects on two effective properties, which is in accordance with Chen et al. [13] hypothesis. According to Nakajima [16], LTPM is characterized by unidirectional straight pores, and the material is considered to be transversely isotropic. Hence, it is possible to consider two distinct properties, i.e., along planes perpendicular and parallel to the direction of pores. Both properties are independent; the property perpendicular to the pore direction can be obtained by numerical homogenization. It is evident, in this case, that the problem can be reduced to a two dimensional (2D) study. The property parallel to the pore direction can be obtained by a simple rule of mixture of the empty pores and the solid body Nakajima [16].

This study aims to improve the well known model of Boccaccini et al [17] which estimates the effect of the void shape on the effective tangent modulus of lotus-type porous medium where the cross section of the pores is considered circular. The picture of Figure 1 shows clearly that the pores have not all circular shape; distinct aspect ratios of elliptical geometry can be observed.

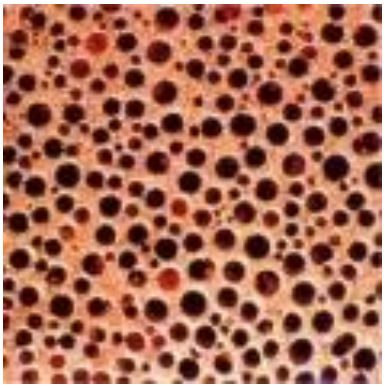

Fig. 1 Loyus-type porous medium

The Boccaccini model will be generalized so that it could take account into elliptical morphology of the pores.

II. MICROSTRUCTURES DESCRIPTION

In this study, considered generated microstructures consisted of a 2D porous matrix containing a random distribution of identical non-overlapping circular or elliptical voids. To highlight the pore morphology effect, five pore shapes are considered *r = 0.2, 0.3, 0.4, 0.5* and *1*.

Where *r* is the ratio between of minor radius and the major radius of the ellipse, See Figure 1, and *r=1* in the circle case.

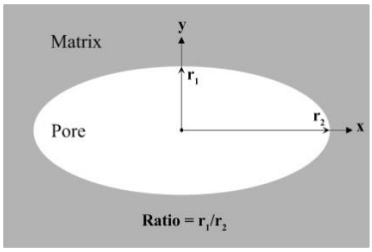

Fig. 1 Pore geometry

For a more complete study, five volume fractions: P = 10%, 20%, 30%, 40% and 50% are considered. Figure 2 illustrates some cases of studied microstructures.

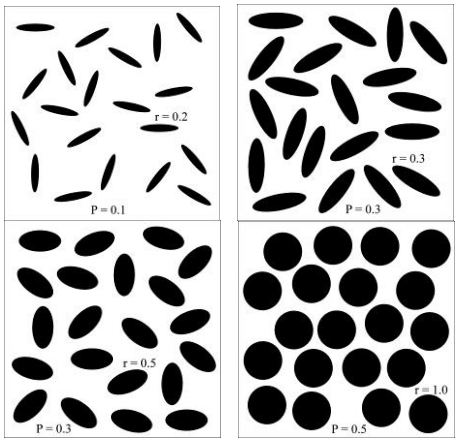

Fig. 2 Studied microstructures examples

It should be noted that the pair (*r* = 0.2, *P* = 50%) is not processed because the configuration is not feasible. The size of each image is 3000x3000 pixel.

III. FINITE ELEMENT MESHING

In this study, a regular mesh technique developped by Lippmann et al., which is widely used in numerical homogenization technique, see Kaddouri et al. [14], Masmoudi et al. [15] and Bourih et al [18], is used. This technique involves superposing a regular finite element grid, Figure 3(a), on a microstructure image, as shown in Figure 3(b). The obtained meshed microstructure, Figure 3(c) was used to attribute the appropriate phase property to each integration point of this regular grid according to the underlying pixel color. Quadratic 8-node elements were considered in this study.

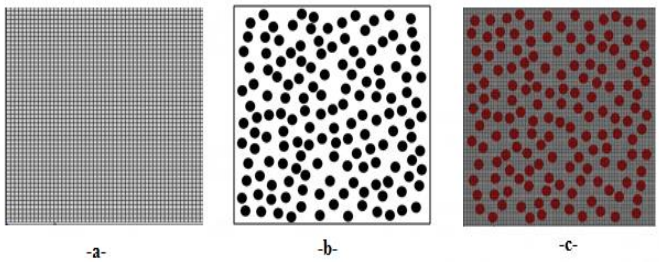

Fig. 3 (a) Finite elements grid, (b) initial microstructure, and (c) meshed microstructure.

To avoid the numerical singularity, the value of the modulus of elasticity E_i of the pores is taken very low $E_i=10^{-7}$ MPa. Subscript *i* indicates inclusion, in this case the pore.

IV. BOUNDARY CONDITIONS

To determine the effective tangent modulus, a simple traction is applied to the different microstructures studied.

Each microstructure is an elastoplastic matrix with modulus of elasticity E_m = 10000 MPa and yield stress R_m = 200 MPa and tangent modulus. Three tangent moduli are considered in this study, $E_{t\ matrix}$ = 476, 910 and 1150 MPa.

IV. NUMERICAL RESULTS AND DISCUSSIONS

This section is devoted to study the effect of the pore shape on the lotus-type porous material effective tangent modulus and to propose a relationship predicting it. The results are obtained using a representative volume element *RVE* = 300 pores.

IV.1 Effective tangent modulus versus pore shape

The results of the effective tangent modulus E_t^{eff} of the microstructure considered for each volume fraction *P*, varying the aspect ratio *r*, are presented in Tables 1, 2 and 3.

Table 1. Effective tangent modulus in terms of r for different volume fractions P ($E_{t\ matrix}$ = 476 MPa)

P [%] / r	10	20	30	40	50
0.2	268.60	154.91	97.29	51.53	-
0.3	304.88	208.88	133.71	87.96	48.86
0.4	331.25	236.88	163.03	99.51	64.86
0.5	346.42	253.77	180.80	118.66	80.85
1	360.26	264.88	195.02	137.77	100

Table 2. Effective tangent modulus in terms of r for different volume fractions P ($E_{t\ matrix}$ = 910 MPa)

P [%] / r	10	20	30	40	50
0.2	529.33	271.87	169.64	86.22	-
0.3	568.88	383.03	236.88	151.93	83.55
0.4	619.11	438.22	295.55	173.77	111.11
0.5	680.46	472.44	329.77	210.66	141.27
1	680.94	491.15	358.95	248.88	179.11

Table 3. Effective tangent modulus in terms of r for different volume fractions P ($E_{t\ matrix}$ = 1150 MPa)

P [%] / r	10	20	30	40	50
0.2	667.11	337.62	210.26	105.80	-
0.3	717.45	479.55	295.55	190.17	102.66
0.4	781.87	552.44	371.11	216.00	136.82
0.5	825.44	598.66	416.96	262.66	176.33
1	857.77	622.39	452.44	313.39	225.44

Five examples of the effective tangent moduluss variations in terms of the aspect ratio ***r*** for different volume fractions P are represented in Figures 4, 5, 6, and 7.

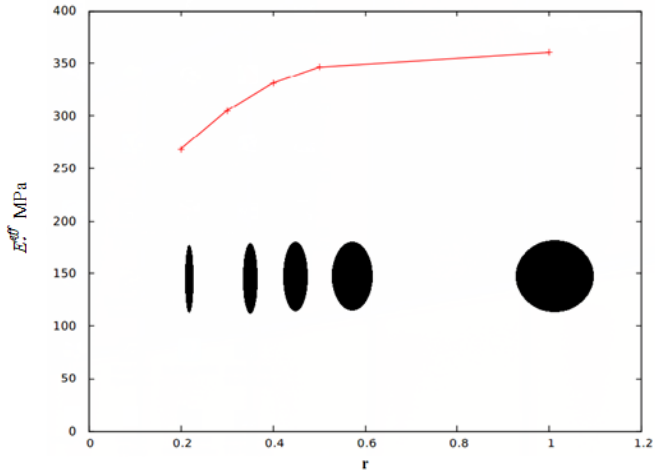

Fig. 4 Effective tangent modulus in terms of r for P = 10%

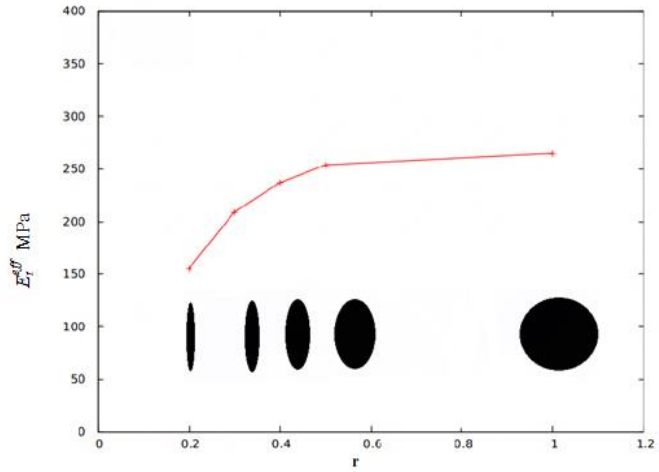

Fig. 5 Effective tangent modulus in terms of r for P = 20%

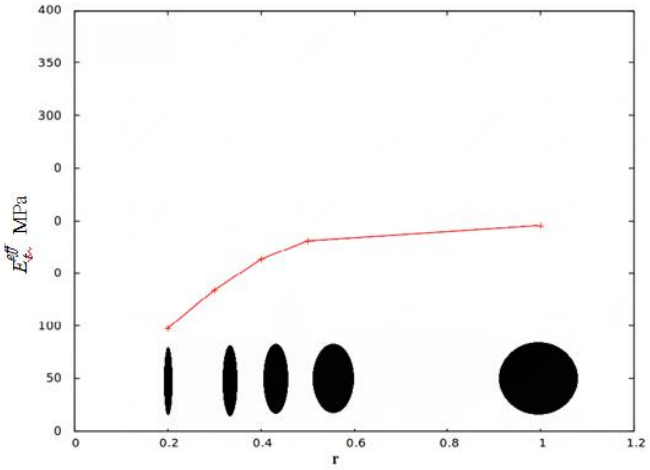

Fig. 6 Effective tangent modulus in terms of r for P = 30%

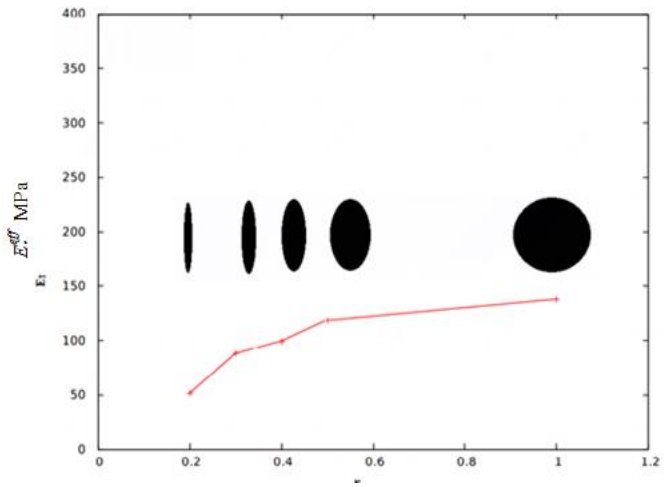

Fig. 7 Effective tangent modulus in terms of r for P = 40%

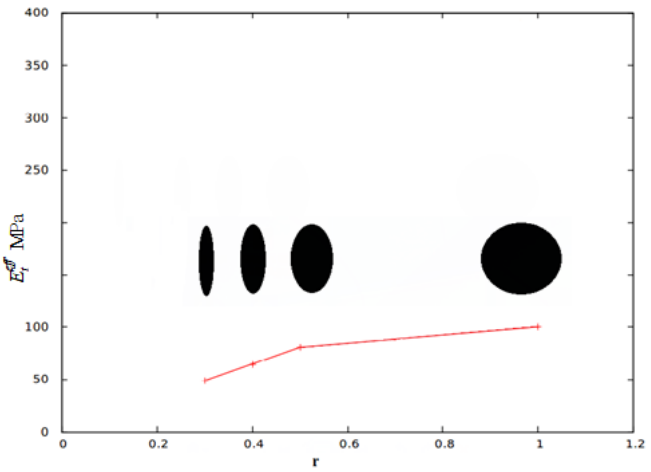

Fig. 8 Effective tangent modulus in terms of r for P = 50%

Figure 9 groups the variations of the effective tangent modulus as a function of the aspect ratio r for the five volume fractions P.

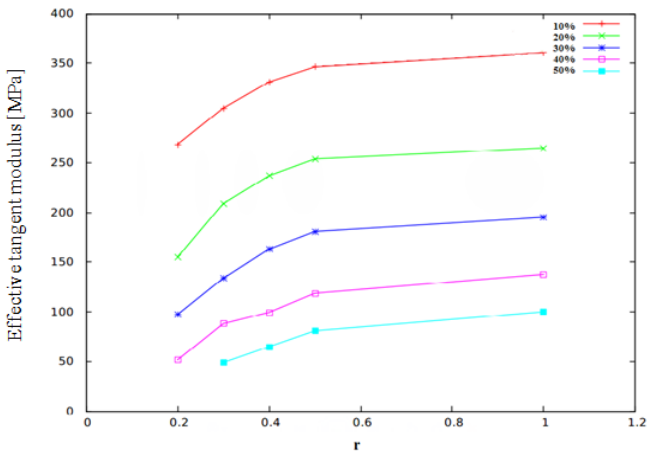

Fig. 9 Effective tangent modulus in terms of r for the five different volume fractions P

Figure 9 shows a variation of the effective tangent modulus E_t^{eff} as a function of the aspect ratio of the pores $\boldsymbol{r}$, when this increases the tangent modulus increases. This proportionality is due to the phenomenon of stress concentration around the pores. The more the aspect ratio increases, the more the pores flatten and consequently the stresses concentrate around the pores.

The phenomenon of stress concentration, around the pores of the stressed microstructure, is illustrated by an example in Figure 10.

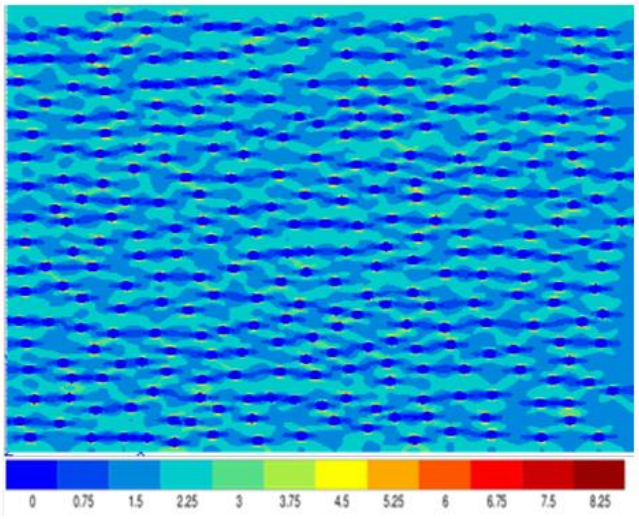

Fig. 10 Stress concentration phenomenon

It is noted that the tangent modulus is inversely proportional to the volume fraction $\boldsymbol{P}$. The increase in the volume fraction combined with the interaction between the pores is at the origin of this behavior.

IV.1 Effective tangent modulus predicting relationship

The objective of this part is to propose a relation to determine the effective tangent modulus for a porous medium, which takes into account the effect of the morphology of the voids. We carried out several fitting tests with the different empirical functions on the points obtained to achieve the best representation of the results. The best representative function is:

$$E_t^{eff} = A.ln(r) + B \qquad (1)$$

All the values of parameters A and B are obtained by fitting the formula and the proposed simulation results are presented in Table 4. These parameters are compared to Boccaccini model.

Table 4. Fitting parameters. $E_{t\ matrix}$ = 476 MPa

P [%]	A	B	$E_t^{\text{Bocaccini}}$
10	56.92	372.63	369.64
20	66.56	282.74	278.62
30	61.28	208.18	202.22
40	52.48	145.51	139.69
50	41.59	102.89	90.18

Table 5. Fitting parameters. $E_{t\ matrix}$ = 909,3MPa

P [%]	A	B	$E_t^{\text{Bocaccini}}$
10	101.94	705.91	706.16
20	132.34	528.41	532.27
30	119.26	383.65	386.32
40	99.43	262.24	266.86
50	78.32	183.85	172.28

Table 6. Fitting parameters $E_{t\ matrix}$ = 1150.66 MPa

P [%]	A	B	$E_t^{\text{Bocaccini}}$
10	123.82	879.45	893.57
20	172.51	670.72	673.53
30	152.97	484.58	488.85
40	126.56	329.55	337.68
50	100.95	231.32	218.01

The first important point concerning the values of the parameter B is that there is a good agreement with the Bocaccini model in the case of the circle.

Therefore, the relatioship (1) can be rewritten as equation (2)

$$E_t^{eff} = A\,ln(r) + E_t^{Boccaccini} \qquad (2)$$

$E_t^{Boccaccini}$ is the effective tangent modulus given by the Bocaccini model.

$$E_t^{Boccaccini} = E_{t\ matrix}\,(1\text{-}P)^{2.4} \qquad (3)$$

The proposed relationship given by equation (2) can be considered as an adjustment of the Bocaccini model which takes into account the effect of pore morphology on the effective tangent modulus of porous media.

The the parameter A can be evaluated by fitting the numerical points represented in Figure 11.

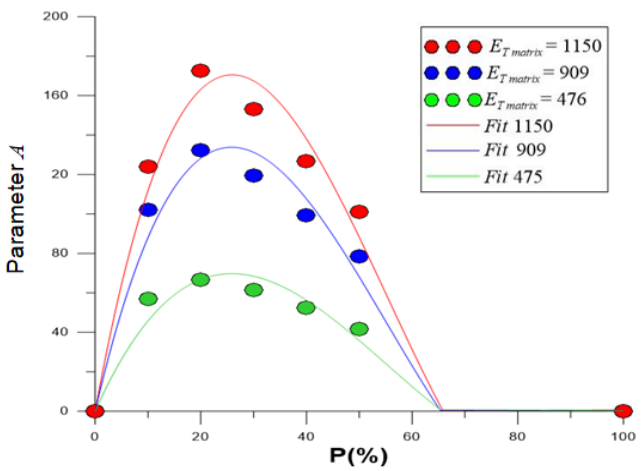

Fig. 11 Parameter A fitting

This is carried out to determine the relation between the parameter A and the volume fraction P. The proposed formula does not ensure the obtaining of the zero bounds. To remedy this problem, two extreme points (P =0%, A=0) and (P=100%, A=0) are added to the simulation results, Figure 11. Thus, the fittage function which gives a better representativeness of these results is given by expression (4)

$$A = aP^3 + bP^2 + cP \qquad (4)$$

The different fitting results are summarized in Table 7.

Table 7. Parameter A fitting results

	$E_{t\ matrix}$ [MPa]		
	476	909.33	1150.66
a	914.00	1765.13	222525
b	-1513.66	-2918.99	-3689.34
c	599.95	1154.24	1464.65

From the results of Table 7, it can be concluded that

$$b \approx -2.5\,c\ ,\ a \approx 1.5c \ \text{ and } \ c \approx 1.3\,E_{t\ matrix} \qquad (5)$$

Also, equation (4) can be written

$$A = (c/2)\,P\left(3P^2 - 5bP + 1\right) \qquad (6)$$

The proposed relationship of equation (1), which estimates the effective tangent modulus of porous medium, takes the final expression given by equation (7)

$$E_t^{eff} = 0.7E_{t\ matrix}\,P\left(3P^2\text{-}5P\text{+}1\right)\,ln(r) + E_T^{Bocaccini} \qquad (7)$$

The comparison between the proposed formula and the simulation results for the different cases studied is illustrated in the Figures 12, 13 and 14.

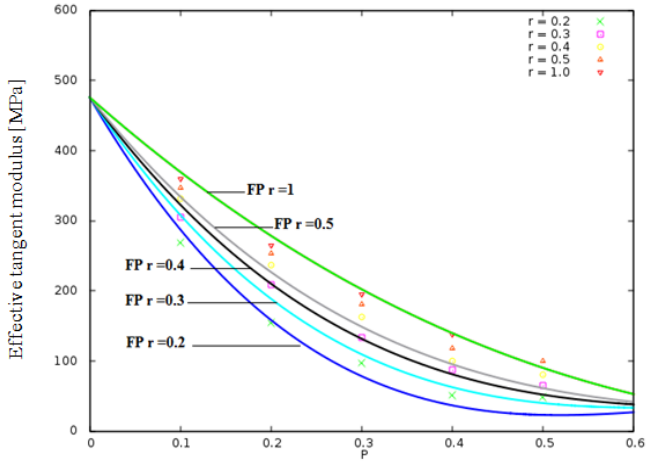

Fig. 12 Compared results with proposed formula
$E_{t\ matrix}$ = 476 Mpa

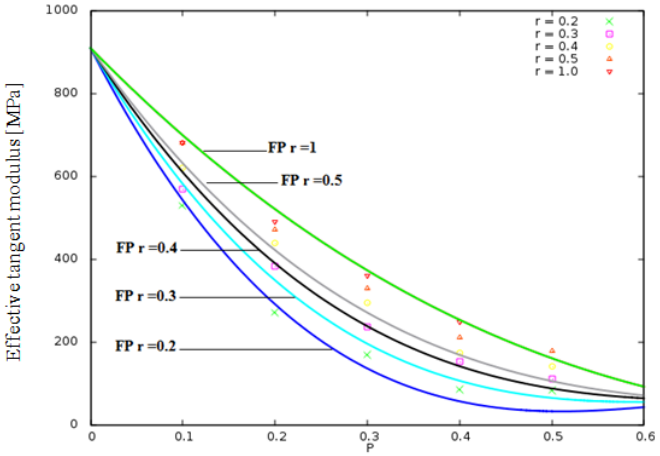

Fig. 13 Compared results with proposed formula
$E_{t\ matrix}$ = 909,33 Mpa

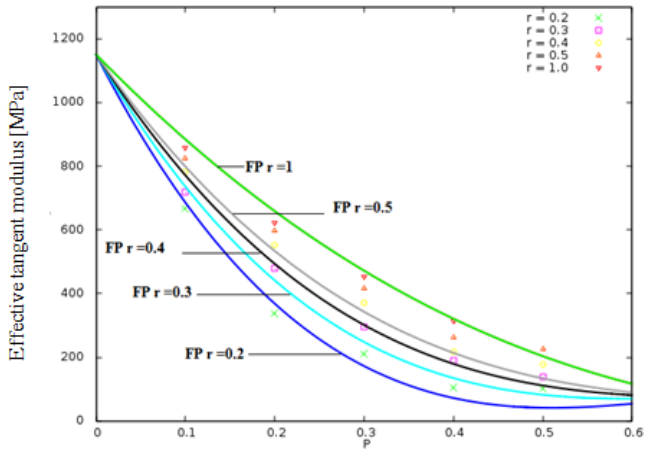

Fig. 14 Compared results with proposed formula
$E_{t\ matrix}$ = 1150,66 Mpa

Figures 12, 13 and 14 show that the numerical results (points) and the proposed formula (curves) are very close, almost superimposed. It also appears a good agreement between the two for different volume fractions *P* and different aspect ratios *r* of the pores.

V. CONCLUSION

The important point of this study was to investigate the effect of the morphology of pores on the effective tangent modulus of lotus-type porous materials. The numerical homogenization technique based on the representative volume element (RVE) was used to estimate the effective studied propety. For this purpose, distinct generated porous microstructures were considered by varying the pore geometry, characterised by its aspect ratio, and by varying the volume fractions of the voids (porosity).

An analytical expression (proposed formula), based on the Bocaccini model has been proposed. A very good agreement has been observed between the numerical results and the proposed formula. This expression can be considered as an improvement of the Bocaccini model which allows the estimation of the effective tangent modulus of porous media while taking into account the effect of pore morphology.

REFERENCES

[1] Nakajima H. Fabrication, properties and application of porous metals with directional pores. Progress in Materials Science 2007, *52*(7), 1091-1173.

[2] Du H, Qi J. Z., Wu J. X., Du S. Q., Xiong T. Y. Structure of porous copper fabricated by unidirectional solidification under pressurized hydrogen. In Materials Science Forum 2010, Vol. 654, pp. 1030-1033. Trans Tech Publications Ltd.

[3] Iio Y, Ide T, Nakajima H. Effect of Transfer Velocity on Porosity of Lotus-type Porous Aluminum Fabricated by Continuous Casting Technique. In Materials Science Forum 2010, (Vol. 658, pp. 211-214). Trans Tech Publications Ltd.

[4] Hyun S. K., Murakami K, Nakajima H. Anisotropic mechanical properties of porous copper fabricated by unidirectional solidification, Materials Science and Engineering : A 2001, 299(1), 241-248.

[5] Ichitsubo T, Tane M, Ogi H, Hirao M, Ikeda T, Nakajima H. Anisotropic elastic constants of lotus-type porous copper: measurements and micromechanics modeling. Acta materialia 2002, *50*(16), 4105-4115.

[6] Hyun S. K., Nakajima H. Anisotropic compressive properties of porous copper produced by unidirectional solidification. Materials Science and Engineering: A 2003, 340(1-2), 258-264.

[7] Tane M, Ichitsubo T, Hirao M, Ikeda T, Nakajima H. Elastic constants of lotus-type porous magnesium: Comparison with effective-mean-field theory.

Journal of applied physics 2004, *96*(7), 3696-3701.
[8] Tane M, Ichitsubo T, Nakajima H, Hyun S. K., Hirao M. Elastic properties of lotus-type porous iron: acoustic measurement and extended effective-mean-field theory. Acta Materialia 2004, 52(17), 5195-5201.
[9] Hyun S. K., Ikeda T. and Nakajima H. Fabrication of lotus-type porous iron and its mechanical properties, Science and Technology of Advanced Materials 2004, 5(1), 201-205.
[10] Xie Z. K., Hyun S. K., Okuda Y, Nakajima H. Measurement and analysis of vibration damping capacity of lotus-type porous magnesium. In Materials science forum 2006, (Vol. 512, pp.325-330). Trans Tech Publications Ltd.
[11] Zaijiu L, Tianwu Y, Qinglin J, Yehua J, Rong Z. Influence of structural parameters on tensile property of gasar porous copper. Rare Metal Materials and Engineering 2014, 43(11), 2609-2613
[12] Liu X, Li Y, Zhang H, Liu Y, Chen X. Effect of pore structure on heat transfer performance of lotus-type porous copper heat sink. International Journal of Heat and Mass Transfer, 144, 118641.
[13] Chen F, Sevostianov I, Giraud A, Grgic D. Evaluation of the effective elastic and conductive properties of a material containing concave pores. International Journal of Engineering Science 2015, 97, 60-68.
[14] Kaddouri W, El Moumen A, Kanit T, Madani S, Imad A. On the effect of inclusion shape on effective thermal conductivity of heterogeneous materials. Mechanics of Materials 2016, 92, 28-41.
[15] Masmoudi M, Kaddouri W, Kanit T, Madani S, Ramtani S, Imad A. Modeling of the effect of the void shape on effective ultimate tensile strength of porous materials: Numerical homogenization versus experimental results. International Journal of Mechanical Sciences 2017, 130, 497-507
[16] Nakajima H, Porous metals with directional pores, Springer 2013
[17] Boccaccini, A. R., Ondracek, G., & Mombello, E. (1996). Determination of stress concentration factors in porous materials. Journal of materials science letters, 15(6), 534-536.
[18] Bourih A, Kaddouri W, Kanit T, Madani S, Imad, A. Effective yield surface of porous media with random overlapping identical spherical voids. Journal of materials research and technology 2018, 7(2), 103-117.